

Orbital Excitations in CMR Progenitor of LaMnO₃ studied by Resonant Inelastic X-ray Scattering

T. Inami^{1,6}, S. Ishihara^{2,6}, H. Kondo³, J. Mizuki^{1,6}, T. Fukuda^{1,6}, S. Maekawa^{3,6},
H. Nakao^{4,6}, T. Matsumura^{5,6}, K. Hirota^{5,6}, Y. Murakami^{5,6}, and Y. Endoh^{3,6}

¹ Synchrotron Radiation Research Center, Japan Atomic Energy
Research Institute (SPring-8), Mikazuki, Hyogo 679-5148, Japan

² Department of Applied Physics, University of Tokyo, Tokyo 113-8656 Japan

³ Institute for Materials Research, Tohoku University, Sendai 980-8577, Japan

⁴ Photon Factory, Institute of Materials Structure Science,
High Energy Accelerator Research Organization, Tsukuba 305-0801, Japan

⁵ Department of Physics, Tohoku University, Sendai 980-8578, Japan and

⁶ Core Research for Evolutional Science and Technology (CREST), Tsukuba 305-0047, Japan

(Dated: received

)

We report resonant inelastic x-ray scattering experiments of the orbital ordered manganite LaMnO₃. When the incident photon energy is tuned near the Mn *K* absorption edge, the spectra reveal three features at 2.5 eV, 8 eV and 11 eV. The 8 eV and 11 eV peaks are considered charge-transfer type excitations. On the other hand, theoretical calculations identify the 2.5 eV peak as an orbital excitation across the Mott gap, *i.e.* an electron excitation from the lower Hubbard band with the $d_{3x^2-r^2}$ and $d_{3y^2-r^2}$ orbital characters to the upper Hubbard band with the $d_{y^2-z^2}$ and $d_{z^2-x^2}$ ones. The observed weak dispersion and characteristic azimuthal angle dependence of this new type of excitations are well reproduced by the theory which includes orbital degeneracy and strong electron correlation.

PACS numbers: 61.10.-i, 75.30.Vn, 71.20.-b, 71.27.+a

The interplay of three degrees of freedom of an electron, *i.e.*, spin, charge and orbital is now a central issue of the perovskite-type manganites showing the colossal magnetoresistance (CMR) which should be potential functional metallic materials in the next generation [1]. LaMnO₃ of the CMR progenitor is a Mott insulator where the electronic configuration of the Mn³⁺ ions is $t_{2g}^3 e_g^1$ with spin quantum number $S = 2$. The band gap appears between two e_g bands of the Mn ions hybridized with the O $2p$ orbitals. The occupied e_g orbitals of $3d_{3x^2-r^2}$ and $3d_{3y^2-r^2}$ are alternately ordered in the ab plane accompanied by the lattice distortion below 780K [2]. With doping of holes in this compound, a variety of electronic phases appear due to the mutual interactions among the multi-degrees of freedom. It is regarded, in fact, that the CMR results from the collapse of a subtle balance under the applied magnetic field destroying the orbital ordered state [3, 4]. Most of the previous explorations on mutual interactions have been directed to spin and lattice dynamics by using various microscopic probes such as neutrons, photons and electrons.

In contrast, little has been explored on dynamics of the orbital degree of freedom. In orbital ordered insulators, the highest occupied and lowest unoccupied electronic states have different orbital characters from each other. Thus, an electron-hole excitation across the Mott gap changes the symmetry of electronic cloud; this is an orbital excitation. It is well known that the virtual orbital excitation between nearest-neighbor transition-metal ions brings about the ferromagnetic superexchange interactions in insulators with alternately ordered or-

bitals [5, 6]. The observed planar ferromagnetic spin alignment in LaMnO₃ signifies that this excitation dominates the low-energy electronic excitation across the Mott gap. The knowledge of the orbital excitations is essential to understand the physics of manganites. Unfortunately, the orbital does not couple directly to most of experimental probes. Therefore, a nature of the orbital dynamics in a wide range of energy and momentum remains to be uncovered, unlike the spin and lattice dynamics.

Recent advances in synchrotron radiation source have changed this situation. We report an exploration of orbital dynamics by high-resolution resonant inelastic x-ray scattering (RIXS). This is an energy and momentum resolving probe [7, 8, 9, 10, 11]. The resonant effects in x-ray diffraction (resonant elastic x-ray scattering) availed recently to detect the orbital ordering in a number of correlated electron systems [2, 12]. By tuning the incident x-ray energy to the absorption edge, scattering becomes dramatically sensitive to the microscopic anisotropy of the electronic clouds. Here, RIXS is applied to the CMR progenitor LaMnO₃. We observed a new peak around the energy transfer 2.5 eV in the orbital ordered state. Its momentum and polarization dependence is entirely distinct from the previous reports on cuprates, which have no orbital degree of freedom [11, 13], but is in accord with a theory including the orbital degeneracy. This new probe would tell us the entire picture of the spin-charge-orbital complex system, *i.e.* CMR manganites.

The experiments were carried out at beam line BL11XU of SPring-8. Incident x rays from a SPring-8 standard undulator were monochromatized by a double-

crystal diamond (111) monochromator, and were focused onto a sample by a horizontally bent mirror. The photon flux and the typical spot size at the sample position were about 2×10^{12} photons/sec and $0.12 \text{ mm(H)} \times 1.4 \text{ mm(V)}$, respectively. The horizontally scattered photons were collected by a spherically bent ($R = 2 \text{ m}$) Ge (531) crystal of diameter 76 mm. The total energy resolution, determined from the quasi-elastic scattering from the sample, was about 0.5 eV full width at half maximum (FWHM) [14]. Two single crystals of LaMnO_3 cut from the same boule were used. One has a [110] direction parallel to the surface normal ($Pbnm$ setting). The other consists of two domains due to twinning, and has a and b axes parallel to the surface normal. All data were taken at room temperature.

The inelastic scattering is plotted in Fig.1 as a function of energy loss for several incident energies (E_i) across the Mn K absorption edge ($= 6.553 \text{ keV}$). From these spectra, resonant nature of the scattering is obvious. Well below and above the absorption edge (spectra a and e), no feature is observed except the elastic scattering at zero energy transfer; the scattering is observed only when the incident energy is close to the absorption edge. The salient spectral features are three peaks at 2.5 eV, 8 eV and 11 eV, as seen in the spectrum c. Note that the resonant energies of the peaks are different from each other. Only the excitation at 2.5 eV is observed in the spectrum d, in addition to the broad scattering of the Mn $K\beta_5$ emission line ($3d \rightarrow 1s$). On the other hand, the 2.5 eV peak vanishes in the spectrum b, while the 8 eV and 11 eV peaks remain. This implies different origins of these three peaks.

The momentum (q) dependence of the inelastic scattering along $\vec{q} = (h, h, 0)$ and $(h, 0, 0)$ is shown in Figs.2 (a) and (b), respectively. Three peaks centered at 2.5 eV, 8 eV and 11 eV seem to show rather flat disper-

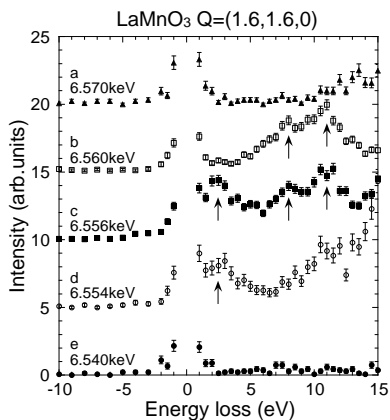


FIG. 1: Inelastic x-ray scattering spectra of LaMnO_3 at $\vec{q}=(1.6,1.6,0)$ for five incident energies near the Mn K edge. Data are offset vertically for clarity. Three features at 2.5 eV, 8 eV and 11 eV are shown by arrows.

sion. The fact is shown more convincingly by the following fitting procedure. Utilizing the fact that the resonant energy of the 2.5 eV peak differs from that of the 8 eV and 11 eV peaks, we extracted low-energy spectra by subtracting data obtained at higher incident energies (6.560 keV for $(h, h, 0)$ and 6.5585 keV for $(h, 0, 0)$) from those obtained at lower incident energies (6.556 keV for $(h, h, 0)$ and 6.5555 keV for $(h, 0, 0)$), and fitted them by a Lorentzian curve. The energy width was fixed in the fitting. The peak position of the 2.5 eV peak obtained is plotted in Figs.2 (c) and (d). The energy dispersion of the 2.5 eV peak is less than a few hundred meV, which should be reexamined by the future measurement with higher energy resolution. We also fitted data measured at $E_i = 6.560 \text{ keV}$ along $\vec{q} = (h, h, 0)$ for the 8 eV and 11 eV peaks. Data were well reproduced by two Lorentzian curves with q independent peak position and line width. The intensity of the 8 eV peak shows weak q dependence, while the intensity of the 11 eV peak largely decreases as q increases.

The 8 eV and 11 eV peaks are considered charge-transfer (CT) type excitations. The 8 eV peak is probably a transition from the O $2p$ orbitals to the unoccupied Mn $3d$ orbitals. In previous RIXS studies on cuprates, CT excitations are observed at about 6 eV. In addition to the similarity in the excitation energy, the weak q dependence of the 8 eV peak in peak position and in integrated intensity agrees well with the reported results about the CT excitation of cuprates [8, 9, 10]. On the other hand,

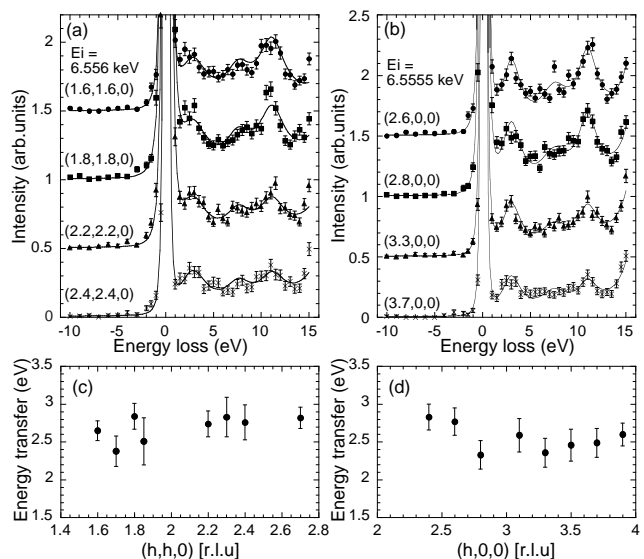


FIG. 2: q -dependence of the resonant x-ray scattering spectra along $\vec{q} = (h, h, 0)$ (a) and $\vec{q} = (h, 0, 0)$ (b) at incident photon energies 6.556 and 6.5555 keV, respectively. Data are offset for clarity. Solid lines are guides to the eye. The peak positions of the 2.5 eV peak obtained from the fitting are also shown ((c) and (d)).

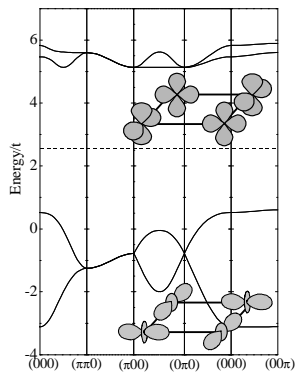


FIG. 3: The electronic band structure for the orbital ordered LaMnO₃. The Hartree-Fock approximation is applied to the generalized Hubbard model where two e_g orbitals and intra-site Coulomb interactions are taken into account. The alternate ordering of the $3d_{3x^2-r^2}$ and $3d_{3y^2-r^2}$ orbitals in the ab plane is assumed. Broken line indicates the chemical potential located at the center of the highest occupied and lowest unoccupied bands. t denotes the hopping integral of electrons between nearest-neighbor $3d_{3z^2-r^2}$ orbitals in the z direction and is about 0.5 – 0.7 eV. The inset shows schematic illustration of the orbital ordered state; the $3d_{y^2-z^2}$ and $3d_{z^2-x^2}$ orbitals (top) constituting the upper Hubbard band and the $3d_{3x^2-r^2}$ and $3d_{3y^2-r^2}$ orbitals (bottom) constituting the lower Hubbard band.

optical conductivity measurements showed that a broad peak exists around 10 eV, which is attributed to transition from the O $2p$ orbitals to the Mn $4s$ or $4p$ orbitals [15]. The 11 eV peak can be ascribed to this transition.

The lowest newly found peak around 2.5eV can be understood in terms of the orbital excitation across the Mott gap, i.e., the electron-hole excitation from the effective lower Hubbard band (LHB) to the upper Hubbard band (UHB). LaMnO₃ is identified as a CT insulator [16]; there exist strong on-site Coulomb interactions in the Mn ion. The insulating gap is formed between UHB consisting of the unoccupied $3d$ orbital and the effective LHB consisting of the O $2p$ orbitals which are strongly mixed with the occupied Mn $3d$ ones. In the orbital-ordered phase, LHB has a symmetry of the $3d_{3x^2-r^2}$ and $3d_{3y^2-r^2}$ orbitals, and UHB has its counterpart, i.e. that of the $3d_{y^2-z^2}$ and $3d_{z^2-x^2}$ orbitals. The excitations from LHB to UHB across the Mott gap (or the CT gap) change the symmetry of the electron wave function.

A theory of RIXS from the orbital excitations is developed on the generalized Hubbard model with orbital degeneracy. Consider the scattering of the incident x rays with momentum \vec{k}_i , energy ω_i and polarization λ_i to \vec{k}_f , ω_f and λ_f . The x-ray scattering cross section [17, 18] is formulated by the Liouville-operator method as [19]:

$$\frac{d^2\sigma}{d\Omega d\omega_f} = \sigma_e \frac{\omega_f}{\omega_i} \sum_{\alpha, \alpha' = x, y, z} (\vec{e}_{k_f \lambda_f})_{\alpha'} (\vec{e}_{k_i \lambda_i})_{\alpha}$$

$$\times (\vec{e}_{k_f \lambda_f})_{\alpha'} (\vec{e}_{k_i \lambda_i})_{\alpha'} \Pi_{\alpha' \alpha}(\omega_i - \omega_f, \vec{k}_i - \vec{k}_f) \quad (1)$$

where $\sigma_e = (e^2/mc^2)^2$ and $\vec{e}_{k\lambda}$ is the polarization of the x rays. The Fourier transform of $\Pi_{\alpha' \alpha}(\omega_i - \omega_f, \vec{k}_i - \vec{k}_f)$ is given by

$$\Pi_{\alpha' \alpha}(t, \vec{r}_{i'} - \vec{r}_i) = \frac{|B|^4}{m^2} \sum_{\gamma \gamma'} D_{\gamma' \alpha'}^* D_{\gamma \alpha} \langle T_{i'x}(t) T_{ix}(0) \rangle, \quad (2)$$

with a constant B and a factor $D_{\gamma\alpha}$ which gives the amplitude of the orbital excitations from the $3d_{\gamma}$ orbital by x ray with polarization α . The orbital degree of freedom is represented by the pseudo-spin operator \vec{T}_i with quantum number $T = 1/2$. $T_z = \pm 1/2$ corresponds to the state where one of the two orbitals is occupied by an electron. Thus, $T_x (\equiv \frac{1}{2}(T_+ + T_-))$ in Eq. (2) implies the orbital excitation. The Jahn-Teller type lattice distortion is introduced in the model and the adiabatic approximation is adopted. This is because the RIXS process is supposed to be faster than the lattice relaxation time. The detailed formulation was presented in Ref. 19. Note that the cross section is represented by the dynamical correlation function of the pseudo-spin operators of orbital. The obtained spectra show a gap about $4t$ and a broad peak centered around $6t$, where t is the hopping integral between the nearest-neighbor $3d_{3z^2-r^2}$ orbitals in the z direction and is about 0.5 – 0.7 eV. The calculated spectra are fitted by a Lorentzian curve. The obtained dispersion of the center of the curve exhibits a weak momentum dependence within $0.1t$. This almost flat dispersion is attributed to the effects of orbital order. The RIXS spectra are approximately given by the convolution of LHB with the $3d_{3x^2-r^2}$ and $3d_{3y^2-r^2}$ orbital characters and UHB with the $3d_{y^2-z^2}$ and $3d_{z^2-x^2}$ ones (see Fig.3). Since the electron hopping between the unoccupied orbitals is forbidden in the ab plane, the dispersion of UHB is almost flat. As a result, the density of state of the LHB dominates the RIXS spectra. This characteristic of the theory based on the orbital excitations is consistent with the experimental results shown in Fig.2.

The significance of the RIXS spectra in the orbital ordered state is that the scattering intensity depends on the azimuthal angle, which is the rotation of the sample about the scattering vector \vec{q} . In the resonant elastic x-ray scattering, this is a direct evidence of the anisotropic scattering factor and is crucial for identifying the scattering from ordered orbitals [12]. The azimuthal angle dependence was measured using the experimental setup shown in Fig.4. The polarization of the incident photon is in the scattering plane (π polarization). When the c axis is perpendicular to the scattering plane, the azimuthal angle ψ is defined as 90° . The integrated intensity of the the 2.5 eV peak at $\vec{q} = (3.4, 0, 0)$ is shown in Fig.4(a) (open circles). The 2.5 eV peak was extracted by subtracting an inelastic spectrum measured at $E_i = 6.560$ keV

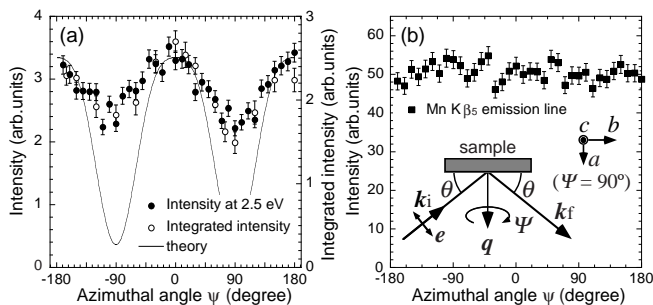


FIG. 4: (a) Azimuthal angle (ψ) dependence of the intensity of the 2.5 eV peak at $\vec{q}=(3.4,0,0)$. Open and solid circles show the integrated intensity of the 2.5 eV peak and the intensity at the energy transfer 2.5 eV, respectively. A solid line shows the integrated intensity of the theoretically calculated RIXS spectra for the orbital ordered LaMnO₃ as a function of ψ . The intensity is scaled so that the maxima approximately agree with the experimental data. (b) Azimuthal angle dependence of the intensity of the Mn $K\beta_5$ emission line at $\vec{q}=(3.4,0,0)$. $E_i = 6.555$ keV and $E_f = 6.5355$ keV. The intensity is independent of ψ . Experimental setup for the azimuthal-angle dependence measurement is shown in inset. The crystal is rotated about the scattering vector $\vec{q}=(3.4,0,0)$. θ is half the scattering angle and was about 34° . At $\psi = 90$ and 0° , the c axis is perpendicular to and in the scattering plane, respectively.

from that measured at $E_i=6.5555$ keV, and was fitted by a Lorentzian curve. The peak position and the width were fixed at 2.4 eV and 3.0 eV (FWHM), respectively, in the fitting. The intensity at the energy transfer 2.5 eV at $\vec{q} = (3.4, 0, 0)$ is also shown by solid circles. Both intensities exhibit a characteristic oscillation with a twofold symmetry and take its maxima at $\psi = 0^\circ$ and 180° . This behavior is in qualitative agreement with the theoretical calculation for the orbital excitation (solid line). The type of the orbital ordered state is the same with those adopted in Fig. 3. A quantitative discrepancy in the oscillation amplitude between the theory and data may be attributed to the multi-domain nature of the sample and the mean-field approximation utilized in the calculation. The similar azimuthal angle dependence was observed for the 8 eV and 11 eV peaks as well. We also measured the Mn $K\beta_5$ fluorescence line, of which intensity is independent of the azimuthal angle (Fig.4(b)). This result illustrates that the observed azimuthal angle dependence does not arise from extrinsic origins, such as anisotropic absorption. Moreover, we would like to emphasize that the azimuthal angle dependence of the 2.5 eV peak is not caused by the shift of the resonant energy. No significant change was observed in the resonant energy of the 2.5 eV peak at $\psi = 0$ and 90° , in sharp contrast to the case of Nd₂CuO₄ [10]. Theoretically, the azimuthal angle dependence originates from the fact that an x -polarized photon does not induce the orbital excitations in a site where the $3d_{3x^2-r^2}$ orbital is occupied, because the local

electronic symmetry at this site is not broken by the x -polarized photon. The observed azimuthal angle dependence strongly supports the present interpretation that the 2.5 eV peak originates from the orbital excitations.

Through the present experimental study of RIXS combined with the theoretical calculation, we were able to identify the inelastic peak at 2.5 eV in LaMnO₃ as the orbital excitations by its momentum and polarization dependence. As a good comparison with the present study, the application to hole doped manganites is promising. Simple metallic behavior without orbital order will result in distinct dispersion of low-energy features. Another possible application of RIXS is to detect the dispersion of collective orbital excitations (orbital waves), which were glimpsed in the recent Raman scattering experiments at zero momentum [20]. As resonant x-ray diffraction study has elucidated static order of orbital in transition metal oxides, RIXS becomes a powerful tool for investigating dynamics of orbital and related phenomena.

We thank T. Iwazumi and T. Arima for helpful discussions, and are grateful to P. Abbamonte for making the diced Ge analyzer. This work was supported in part by Grant-in-Aid for Scientific Research Priority Area from the Ministry of Education, Science, Sport, Culture and Technology of Japan, and Science and Technology Special Coordination Fund for Promoting Science and Technology of Japan.

-
- [1] Y. Tokura and N. Nagaosa, *Science* **288** 462 (2000).
 - [2] Y. Murakami *et al.*, *Phys. Rev. Lett.* **81**, 582 (1998).
 - [3] *Colossal Magnetoresistance Oxides*, edited by Y. Tokura, (Gordon and Breach, Amsterdam, 2000).
 - [4] *Physics of Manganites*, edited by T. Kaplan and S. D. Mahanti, (Plenum Publishers, 1999).
 - [5] J. B. Goodenough, *Phys. Rev.* **100**, 564 (1955).
 - [6] J. Kanamori, *J. Phys. Chem. Sol.* **10**, 87 (1959).
 - [7] P.M. Platzman and E.D. Isaacs, *Phys. Rev. B* **57**, 11107 (1998).
 - [8] P. Abbamonte *et al.*, *Phys. Rev. Lett.* **83**, 860 (1999).
 - [9] J. P. Hill *et al.*, *Phys. Rev. Lett.* **80**, 4967 (1998).
 - [10] K. Hämäläinen *et al.*, *Phys. Rev. B* **61**, 1836 (2000).
 - [11] M. Z. Hasan *et al.*, *Science* **288**, 1811 (2000).
 - [12] Y. Murakami *et al.*, *Phys. Rev. Lett.* **80**, 1932 (1998).
 - [13] K. Tsutsui *et al.*, *Phys. Rev. Lett.* **83**, 3705 (1999).
 - [14] T. Inami *et al.*, *Nucl. Instr. and Meth. A* (2001), in press.
 - [15] T. Arima and Y. Tokura, *J. Phys. Soc. Jpn.* **64**, 2488 (1995).
 - [16] T. Saitoh *et al.*, *Phys. Rev. B* **51**, 13942 (1995).
 - [17] M. Blume, *J. Appl. Phys.* **57** 3615 (1985).
 - [18] Y. Ma, in *Raman Emission by X-ray Scattering*, edited by D. L. Ederer and J. H. McGuire (World Scientific, New Orleans, 1996), pp. 32-40.
 - [19] H. Kondo *et al.*, *Phys. Rev. B* **64**, 014414 (2001).
 - [20] E. Saitoh *et al.*, *Nature* **410**, 180 (2001).